

Exploring Λ - and Ξ -triton correlation functions in heavy-ion collisions

Faisal Etminan*

*Department of Physics, Faculty of Sciences,
University of Birjand, Birjand 97175-615, Iran and
Interdisciplinary Theoretical and Mathematical Sciences
Program (iTHEMS), RIKEN, Wako 351-0198, Japan*

(Dated: December 11, 2024)

In this work, Λ -triton(t) momentum correlation functions, to be measured in high-energy heavy-ion collisions, are explored. Mainly, STAR detector acquired data for Au+Au collisions at $\sqrt{s_{NN}} = 3$ GeV provides an opportunity to explore the Λt correlation function. A Kurihara's isle-type and spin-averaged Λt potential is employed. The strengths of Λt potential is tuned in a such way to reproduce the experimental ground state energy of ${}^4_{\Lambda}H$ ($\Lambda + t$). Since the new measurements by the STAR Collaboration present a significant increase in the Λ binding energy of the hypertriton and ${}^4_{\Lambda}H$ hypernuclei, I investigate the sensitivity of correlation function by strengthen the Λt potential. Besides, even though there is no experimental data on the Ξ -triton interaction yet, an estimate of its momentum correlation functions by taking Ξ -triton potential from the literature is given.

I. INTRODUCTION

Baryons containing strange quarks, called hyperon, and if a Λ hyperon replaces one of the nucleons ($N = n$ or p) in the nucleus, the possible bound state that it is made of the hyperon and core of the remaining nucleons are known as Λ hypernucleus. The light hypernuclei are ideal systems for testing the hyperon-nucleon (YN) interactions, and they have been the subject of many studies over the last three decades or so [1–5].

The binding energy of Λ hyperon B_{Λ} , i.e. the Λ separation energy for a hypernuclei,

* fetminan@birjand.ac.ir

is characterized by the mass difference between the hypernucleus, and the sum of the nucleon core and the Λ . The binding energies of hypernuclei are investigated by sophisticated theoretical method such as cluster models [6], exact Faddeev or Yakubovsky equations [7–10], no-core shell model [11] based on the interactions constructed in the meson-exchange picture [12], chiral effective field theory [13] or lattice quantum chromodynamics simulations [10, 14].

New measurements by the STAR (Solenoidal Tracker at RHIC) Collaboration at RHIC (Relativistic Heavy Ion Collider) shows a significant increase in the Λ binding energy of the hypertriton [4], in fact some of the past values have been called into question [15]. Therefore, the accurate measurements of Λ binding energies of heavier hypernuclei than the hypertriton are supposed to make progress our knowledge about the Λ interactions by heavier nuclei.

The ${}^4_{\Lambda}H$ nucleus, a bound state of a Λ hyperon and a tritium core, is an isotope of the hydrogen. It was observed in the primary helium bubble chamber and nuclear emulsion experiments [16]. So far the binding energy of ${}^4_{\Lambda}H$ is measured by different experimental techniques such as the emulsion technique [16], decay-pion spectroscopy in electron scattering [17], high-resolution decay-pion spectroscopy by A1 Collaboration at the Mainz Microtron MAMI, Germany [18] and very recently, it is measured in Au+Au collisions at $\sqrt{s_{NN}} = 3$ GeV by the STAR Collaboration [4, 5].

Since studying YN interactions by the classical scattering experiments is challenging, recent progress in theoretical and experimental techniques in heavy-ion reactions at relativistic energies provide a unique opportunity to explore YN interactions through measuring two-particle correlations [19, 20] and production of light hypernuclei [5]. The first measurement of Λp and Λd correlation, which is done by STAR Collaborations with $\sqrt{s_{NN}} = 3$ GeV Au+Au collisions [21], shed light on both YN two-body and YNN three-body interactions [20, 22–24], which is crucial for understanding neutron star properties. The correlation functions for some hadron-deuteron systems are explored theoretically, such as pd [23, 25, 26], K^-d [24, 26], Λd [20, 27], Ξd [28], and ΩNN [29, 30]. Moreover very recently, the momentum correlation between $\Lambda\alpha$ [31], $\Xi\alpha$ [32], $\Omega\alpha$ [33] and $\phi\alpha$ [34] have been investigated theoretically.

According to the above discussion, it is desirable to predict the Λt momentum correlation functions numerically using phenomenological potentials to be compared by expected measuring Λt correlations function by STAR in the relativistic heavy ion collisions [4] as an

independent source of information.

Besides, I explored the formation possibility of Ξ - t system by evaluating its momentum correlation functions applying an effective folding Ξ - t potential from the literature [35]. However, no experimental results or observations have been reported about Ξ - t system so far, but evidence from femtoscopic measurements for an attractive Ξ^-p interaction [36] have triggered significant motivation to investigate Ξ hypernuclei theoretically [11, 37].

The paper is structured as follows: In Sec. II, the employed potentials in this work, i.e., the effective two-body Λt and Ξ^-t potentials, are described, and some properties are discussed. The correlation function results by Koonin-Pratt (KP) formula [38] are given in Sec. III and the relevant discussions about the results also presented there. I summarize and conclude my work in Sec. IV.

II. EFFECTIVE TWO-BODY Λt AND Ξ^-t POTENTIALS

For the Λt potential, Kurihara's isle-type potential is employed [39]. That is extracted from Dalitz's hard core ΛN interaction and has a two-range Gaussian form [40]. The strength of Λt potential is tuned in such a way as to reproduce the experimental ground state energy of ${}^4_{\Lambda}H$, $E = -2.04(4)$ MeV for the singlet (S) Λt state [16] and the first excited state energy, $E = -0.99(4)$ MeV for the triplet (T) Λt state [11, 41]. $U_{\Lambda t}(r)$ potential between t and Λ is given by [35]

$$U_{\Lambda t}(r) = \frac{1}{4}V_{\Lambda t}^S(r) + \frac{3}{4}V_{\Lambda t}^T(r) = \quad (1)$$

$$359.2 \exp \left[- \left(\frac{r}{1.25} \right)^2 \right] - 324.9 \exp \left[- \left(\frac{r}{1.41} \right)^2 \right],$$

this Isle potential has a two-range Gaussian form with the central repulsion and the long range attraction and it is shown in Fig. 1.

Furthermore, the new Λ binding energies measurements, performed for the ${}^4_{\Lambda}H$ (0^+) state with respect to the ${}^3H + \Lambda$ mass are, $2.12(1)_{\text{stat.}}(9)_{\text{syst.}}$ MeV [17], $2.157(5)_{\text{stat.}}(77)_{\text{syst.}}$ MeV by A1 Collaboration [18] and $2.22(6)_{\text{stat.}}(14)_{\text{syst.}}$ MeV by the STAR Collaboration [4]. Since the new measurements (especially by the STAR Collaboration) show a significant enhancement in the Λ binding energy of the hypertriton and ${}^4_{\Lambda}H$ hypernuclei, and also to check the sensitivity of the correlation function to the nature of Λt interaction, the

strengthened potential, $U_{\Lambda t}^+$ is defined as

$$U_{\Lambda t}^+(r) = 1.2 U_{\Lambda t}(r). \quad (2)$$

The strength of the original (old) potential in Eq. (1) is increased by 20 percent. To compare with $U_{\Lambda t}$ the behavior of this potential is depicted in Fig. 1 as function of the distance between t and Λ .

In the case of Ξ^-t system, the following folding potential, taken from Ref. [35], has been used,

$$U_{\Xi^-t}(r) = \sum_{i=1}^3 c_i e^{-(r/d_i)^2}, \quad (3)$$

the potential parameters are $(c_1, c_2, c_3) = (103.67, -51.57, -44.10)$ MeV and $(d_1, d_2, d_3) = (1.362, 1.568, 1.610)$ fm. $U_{\Xi^-t}(r)$ is built by folding an effective ΞN potential with the triton density distribution function $\rho(r')$ [35, 42],

$$U_{\Xi^-t}(r) = \int d\mathbf{r}' \rho(r') \bar{V}_{\Xi^-N}(\mathbf{r} - \mathbf{r}'), \quad (4)$$

where r is the distance of Ξ^- from the centre-of-mass of the triton. The nucleon density in the triton is evaluated from a harmonic oscillator model,

$$\rho(r) = 3 \left(\frac{3\beta}{2\pi} \right)^{3/2} \exp\left(-\frac{3}{2}\beta r^2\right), \quad (5)$$

$\beta = 0.386 \text{ fm}^{-2}$ is the strength of harmonic oscillator that reproduces the matter root-mean-square (rms) radius 1.61 fm which is measured in electron scattering experiments from light nuclei [43]. The effective potential \bar{V}_{Ξ^-N} is approximated from the isospin-spin averaged Ξ^-N interaction,

$$\bar{V}_{\Xi^-N} = \frac{1}{8} V_{\Xi^-p}^{1S_0} + \frac{3}{8} V_{\Xi^-p}^{3S_1} + \frac{1}{8} V_{\Xi^-n}^{1S_0} + \frac{3}{8} V_{\Xi^-n}^{3S_1}, \quad (6)$$

the two-body potential V_{Ξ^-N} between Ξ^- and N are Shinmura's potential [35] which is based on the Nijmegen model-D potential[44, 45]. The low-energy data derived with $U_{\Xi^-t}(r)$ indicates no bound or resonant state.

The binding energy and scattering observables for Λ (Ξ) - t systems are obtained by solving two-body Schrödinger equation using $U_{Yt}(r)$ potentials (plotted in Fig. 1) as the input. In our numerical calculations, the masses of Λ and Ξ^- , $m_\Lambda = 1115.683$ MeV and $m_{\Xi^-} = 1321.71$ MeV is taken from the PDG [46], and the masses of triton $m_t = 2808.921$ MeV is from CODATA [47]. The results for scattering length, effective range, and binding energy are

TABLE I: Scattering length a_0 , effective range r_0 and binding energy B_Y for Λt and Ξt systems. In the case of Ξt interaction, the binding energy by including Coulomb interaction is given between parentheses, it implies that $\Xi^- t$ system could be a Coulomb-assisted bound state [37]. The potentials $U_{\Lambda t}(r)$ and $U_{\Xi^- t}(r)$ are taken directly from Ref. [35]. Here, the NB is an acronym for No Bound or resonance states.

Model	a_0 (fm)	r_0 (fm)	B_Y (MeV)
$U_{\Lambda t}(r)$	5.9	2.3	1.27
$U_{\Lambda t}^+(r)$	4.6	2.1	2.57
$U_{\Xi^- t}(r)$	-125.0	3.1	NB(0.17)

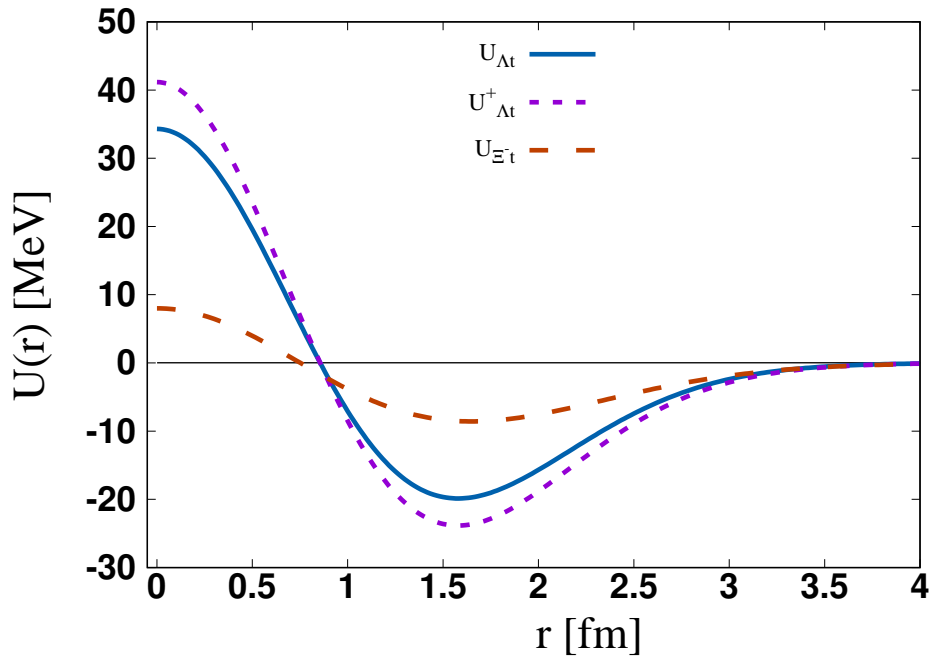


FIG. 1: The potentials $U_{Yt}(r)$ as functions of distance between Y (Λ, Ξ) and triton. $U_{\Lambda t}$ (solid blue line) is given by Eq. (1) and $U_{\Lambda t}^+ = 1.2 U_{\Lambda t}$ (dotted violet line) simulates a 20 percent increment in Λt interaction. The Ξt folding potential in Eq. (3) is shown by $U_{\Xi^- t}$ (dashed dark-orange line).

given in Table I. With these values of masses in this analysis, the binding energies of ${}^4_{\Lambda}H$ by $U_{\Lambda t}(r)$ and $U_{\Lambda t}^+(r)$ are 1.27 and 2.57 MeV, respectively. But, the Ξt potential supports only a Coulomb-assisted bound state by values of 0.17 MeV.

Moreover, the relevance Yt phase shifts (δ/π) as functions of the relative momentum ($q = \sqrt{2\mu E}$ where μ is the reduced mass of Yt system) is shown in Fig. 2. The obtained phase shifts shows attractive behavior for all interactions. Low-energy part of Yt phase shifts in Fig. 2 defines scattering length a_0 and effective range r_0 employing the effective range expansion (ERE) formula,

$$q \cot \delta = -\frac{1}{a_0} + \frac{1}{2}r_0q^2 + \mathcal{O}(q^4). \quad (7)$$

The numerical results for $U_{\Lambda t}$ in Eq. (1), $U_{\Lambda t}^+$ in Eq. (2) and Ξt folding potential in Eq. (3) are listed in table I.

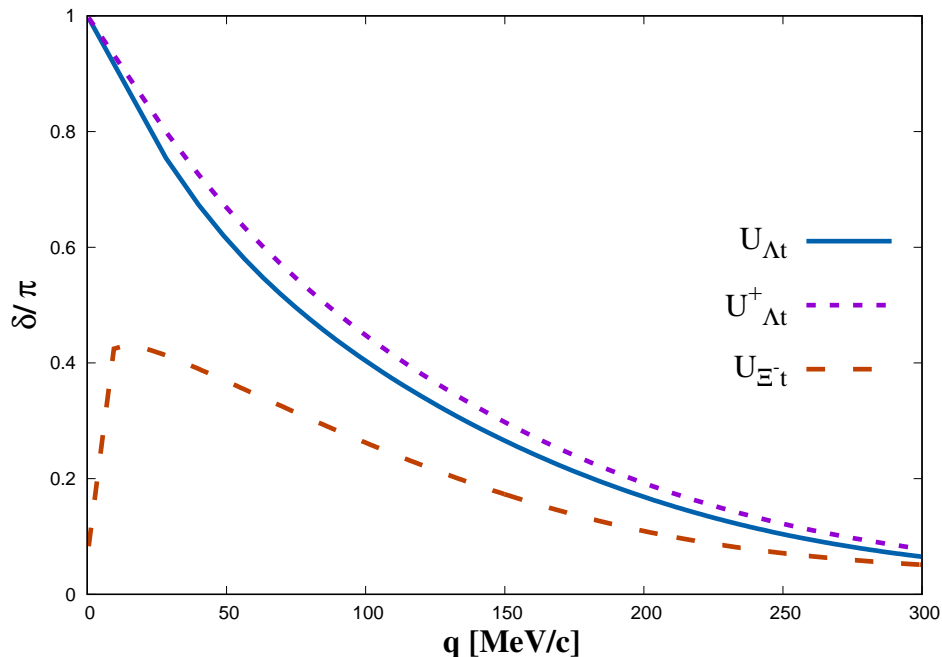


FIG. 2: Λt and Ξt normalized phase shifts as functions of the relative momentum q using $U_{\Lambda t}$ (solid blue line), $U_{\Lambda t}^+$ (dotted violet line) and $U_{\Xi t}$ (dashed dark-orange line).

III. CORRELATION FUNCTION RESULTS AND DISCUSSION

The two-particle correlation produced in a collision [19, 38, 48–50] presents valuable information about the space-time evolution of the particle-emitting source and final state interactions entail hyperons [51]. The Yt correlation function is given in terms of the two-particle distribution $N_{Yt}(\mathbf{k}_Y, \mathbf{k}_t)$ normalized by the product of the single particle distribu-

tions, $N_Y(\mathbf{k}_Y) N_t(\mathbf{k}_t)$,

$$C(\mathbf{k}_Y, \mathbf{k}_t) \equiv \frac{N_{Yt}(\mathbf{k}_Y, \mathbf{k}_t)}{N_Y(\mathbf{k}_Y) N_t(\mathbf{k}_t)}, \quad (8)$$

where the \mathbf{k}_Y and \mathbf{k}_t are the momentum of particle Y and triton. In the experiments, correlation function is measured by

$$C(q) = \mathcal{N} \frac{A(\mathbf{q})}{B(\mathbf{q})} = \int 4\pi r^2 dr S(\mathbf{r}) \left| \Psi_{Yt}^{(-)}(\mathbf{r}, \mathbf{q}) \right|^2, \quad (9)$$

that is equivalent to Eq. (8). Where $\mathbf{q} = (m_Y \mathbf{k}_Y - m_t \mathbf{k}_t) / (m_Y + m_t)$ is the relative momentum, and $A(\mathbf{q})$ is the distribution of q with both particles from the same event, $B(\mathbf{q})$ is for two particles from different events, and \mathcal{N} is the normalization factor. The right-hand side of Eq. (9) is known as by the Koonin-Pratt (KP) formula [38]. $S(r) = \exp(-r^2/4R^2) / (2\sqrt{\pi}R)^3$ with source size R is known as the source function, which defines the distribution of the relative distance of particle pairs, and is assumed to be spherical and static Gaussian in my calculations. $\Psi_{Yt}^{(-)}$ is the relative wave function of the particle pairs that can be obtained straightforwardly by solving a two-body Schrödinger equation for a given Yt potential.

The Λt correlation functions for three different source sizes, $R = 1, 3$ fm and 5 fm using $U_{\Lambda t}$ and $U_{\Lambda t}^+$ are shown in Fig. 3 a) , b) and c), respectively. The sizes of the sources have been chosen according to the sizes that are usually people used in the exploration of two-hadron correlation functions [31–33]. The particular dip shape can be observed at small source size $R = 1$ fm, that is conventional in the bound state of system near the threshold [31]. Moreover, Fig. 3 a) shows the results for all cases of two potentials are different at low momentum $q \lesssim 100$ MeV/c. According to Fig. 1 the $U_{\Lambda t}$ potential model, is more attractive than $U_{\Lambda t}^+$ potential, thus it gives enhancement of $C_{\Lambda t}(q)$. Nevertheless, with the increase of the source size, the difference between the $C_{\Lambda t}(q)$ s decreases until they are almost identical for $R = 5$ fm. As a consequence, the future measurements of Λt correlation functions in the relatively low momentum region with small radius of the sources, can be used as a probe to study the Λt interaction in dense matter.

The Ξt correlation functions using $U_{\Xi-t}$ in Eq. (3) for three different source sizes are presented in Fig. 4. In this case, the Coulomb potential is also included. It is seen a substantial enhancement in Ξt correlation at low momentum region. That implies a relatively large scattering length value about $a_0 \approx 125$ fm (as given in table I) and the Coulomb attraction. In order to see the effect of strong interaction, the pure Coulomb potential is

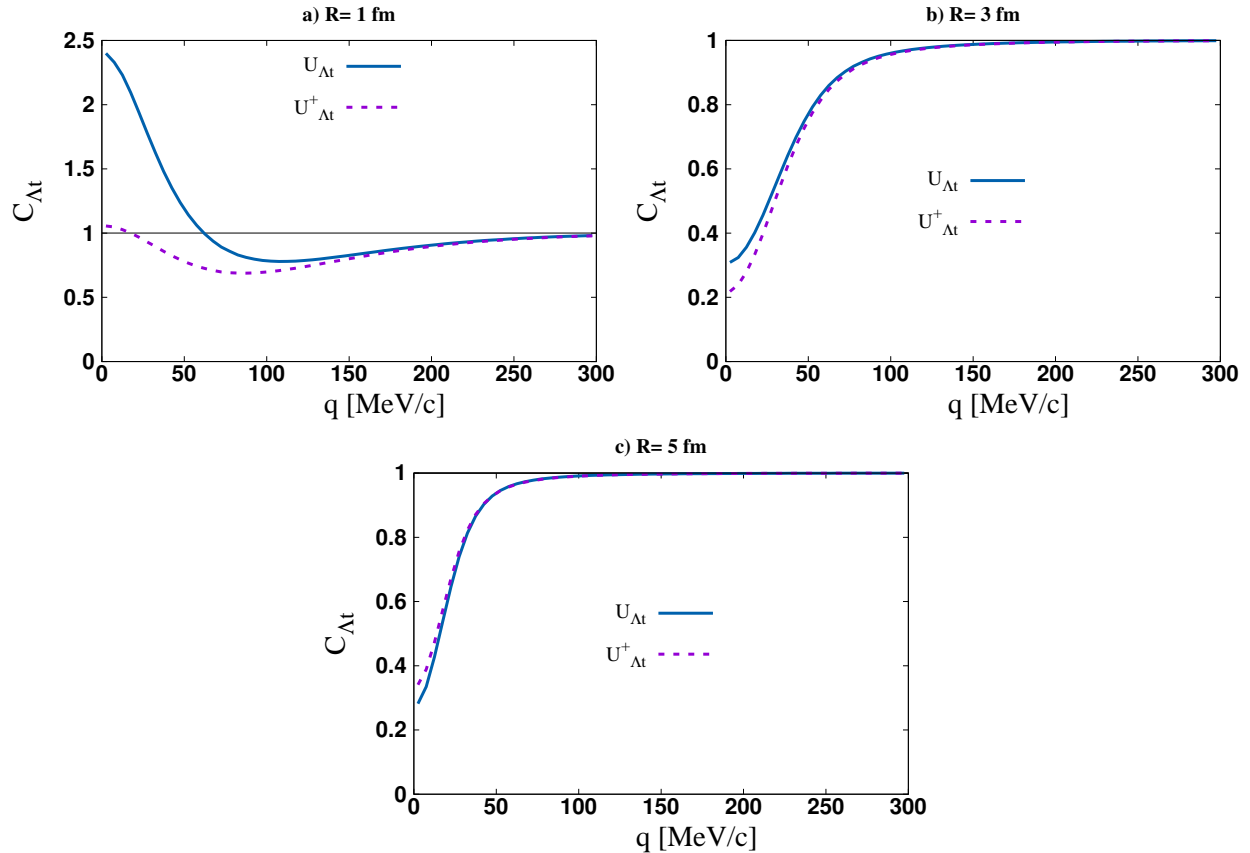


FIG. 3: Λt correlation functions using $U_{\Lambda t}$ (solid blue line), $U_{\Lambda t}^+$ (dotted violet line) for three different source sizes: a) $R = 1$ fm, b) $R = 3$ fm and c) $R = 5$ fm.

plotted in Fig. 4 (black solid line). Specifically, Ξ^-t correlation functions are enhanced at the small source and suppressed at the significant source analogous to the pure Coulomb calculation. Moreover, the difference between Ξ^-t correlation function and pure Coulomb result, which is embodied as a dependency of the correlation function on the size of the source, it implicitly implies the existence of a Coulomb-assisted bound state [32].

IV. SUMMARY AND CONCLUSIONS

In this exploratory study, Λ and Ξ -triton correlation functions in heavy-ion collisions were predicted. They can be measured in the STAR detector at RHIC [4] by employing the femtoscopy technique.

For Λt two-body potential, Kurihara's isle-type potential [39], that is extracted from Dalitz's hard core ΛN interaction is used. The strength of Λt potential is tuned in such a

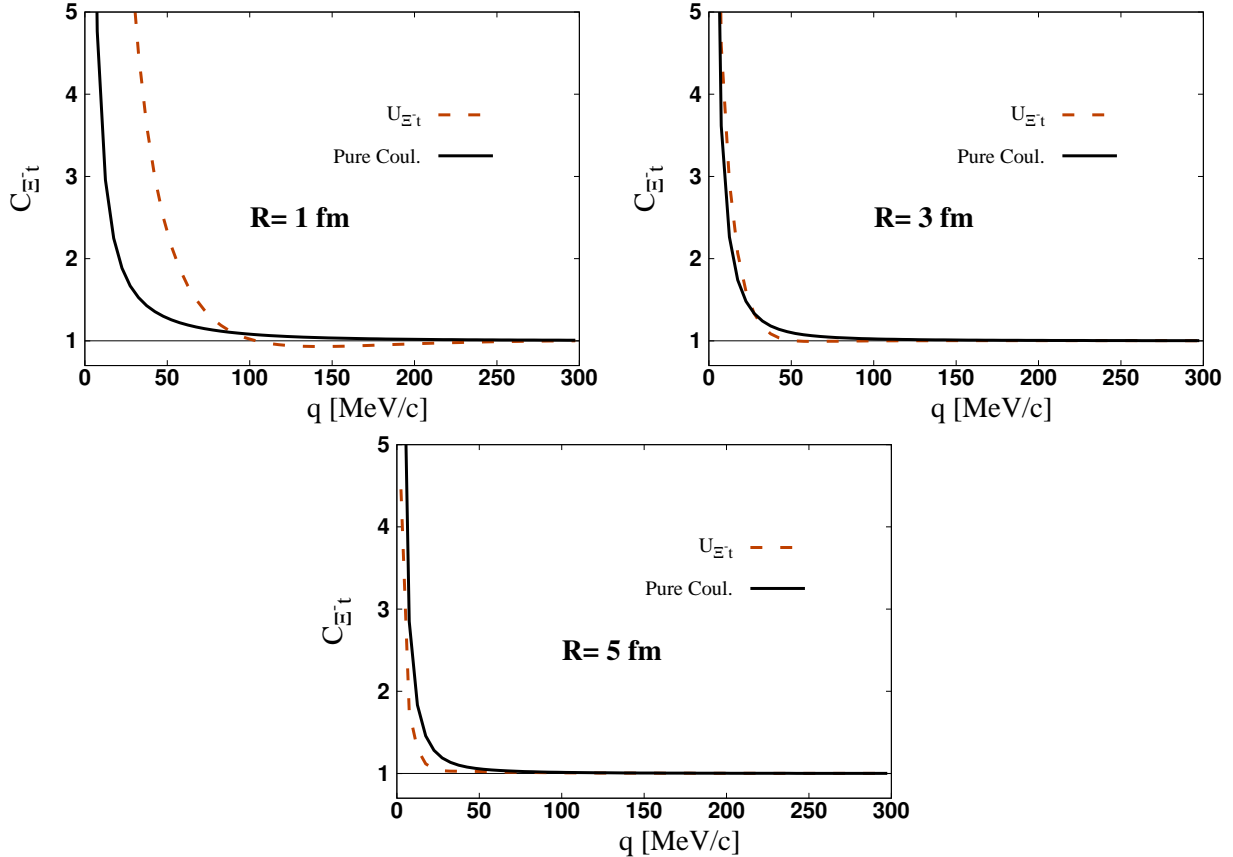


FIG. 4: Ξ^-t correlation functions using U_{Ξ^-t} in Eq. (3) for three different source sizes: $R = 1, 3$ and $R = 5$ fm, when the Coulomb interaction is switched on. For comparison, the pure Coulomb result, where the strong interaction is switched off, is presented by the solid black line.

way as to return the experimental ground state energy of ${}^4_{\Lambda}H$ [16, 41]. In addition, since the new measurements show a relatively significant increase in the Λ binding energy of the hypertriton and ${}^4_{\Lambda}H$ hypernuclei [4, 17, 18], I also performed the calculations with an increased strength of Λt potential by about twenty percent.

And for Ξ^-t two-body potential, because there is no experimental measurement on the Ξ^-t interaction yet, I took an effective folding potential from the literature [35] which is based on the Nijmegen model-D ΞN potential[44, 45]. It returns the large scattering length without a bound state (a shallow Coulomb-assisted bound state) in the Ξ^-t (Ξ^-t) channel.

Employing these Yt potentials, correlation functions are calculated using the KP formula for three different source sizes, $R = 1, 3$ fm and 5 fm, where the choice is motivated by values suggested by analyses of measurements of the two-hadron correlation function in pp

collisions and heavy ion collisions [31, 32]. It is remarkable that the KP formula in Eq. (9) is accurate under the condition that two correlated particles can be treated as point-like objects. The source size of the composite particle t should be bigger than those with single hadron emissions, for the reason that, there is a probability of t particle formation by the coalescence of three nucleons emitted from the fireball [25, 26, 52]. Therefore, we rather deal with a four-body scattering problem of a three nucleons and a hyperon. In the other hand, a formation of triton and production of Λt correlation arise at same time. Essentially, this mechanism must be taken into account in future studies and it is beyond the scope of this paper.

The numerical results of this work suggest that measurements of the Λt momentum correlation function in heavy-ion collisions [4, 5] look indeed very promising. Particularly, collected data by the STAR detector from Au+Au collisions at a center-of-mass energy of $\sqrt{s_{NN}} = 3$ GeV provide an opportunity to study the Λt correlation function.

In conclusion, the results presented here for Ξ - t momentum correlation functions were obtained by using the old Ξ - t interaction [35]. For an accurate comparison with future experimental data, I have a plan to investigate this system theoretically using different modern ΞN potentials [11, 37] in the future.

ACKNOWLEDGEMENT

I am grateful to the authors and maintainers of ”*Correlation Analysis tool using the Schrödinger Equation*” (CATS) [53, 54], a modified version of which is used for calculations in this exploratory study. Discussions during the long-term workshop, HHIQCD2024, at Yukawa Institute for Theoretical Physics (YITP-T-24-02), aroused in me the motivation for this work.

-
- [1] H. Nemura, Y. Akaishi, and Y. Suzuki, Ab initio Approach to s -Shell Hypernuclei ${}^3_{\Lambda}\text{H}$, ${}^4_{\Lambda}\text{H}$, ${}^4_{\Lambda}\text{He}$, and ${}^5_{\Lambda}\text{He}$ with a ΛN - ΣN Interaction, *Phys. Rev. Lett.* **89**, 142504 (2002).
- [2] A. Gal, E. V. Hungerford, and D. J. Millener, Strangeness in nuclear physics, *Rev. Mod. Phys.* **88**, 035004 (2016).

- [3] L. Adamczyk *et al.* (STAR Collaboration), Measurement of the ${}^3_{\Lambda}\text{H}$ lifetime in Au+Au collisions at the BNL Relativistic Heavy Ion Collider, *Phys. Rev. C* **97**, 054909 (2018).
- [4] M. Abdallah *et al.*, Measurement of ${}^4_{\Lambda}\text{H}$ and ${}^4_{\Lambda}\text{He}$ binding energy in Au+Au collisions at $s_{NN} = 3$ GeV, *Phys. Lett. B* **834**, 137449 (2022).
- [5] M. Kozhevnikova and Y. B. Ivanov, Light Hypernuclei Production in Au+Au Collisions at $\sqrt{s_{NN}} = 3$ GeV within Thermodynamic Approach (2024), arXiv:2401.04991 [nucl-th].
- [6] E. Hiyama, M. Kamimura, T. Motoba, T. Yamada, and Y. Yamamoto, $\Lambda - \Sigma$ conversion in ${}^4_{\Lambda}\text{He}$ and ${}^4_{\Lambda}\text{H}$ based on a four-body calculation, *Phys. Rev. C* **65**, 011301 (2001).
- [7] K. Miyagawa, H. Kamada, W. Glöckle, and V. Stoks, Properties of the bound $\Lambda(\Sigma)\text{NN}$ system and hyperon-nucleon interactions, *Phys. Rev. C* **51**, 2905 (1995).
- [8] A. Nogga, H. Kamada, and W. Glöckle, The Hypernuclei ${}^4_{\Lambda}\text{He}$ and ${}^4_{\Lambda}\text{H}$: Challenges for Modern Hyperon-Nucleon Forces, *Phys. Rev. Lett.* **88**, 172501 (2002).
- [9] F. Etminan and S. F. Farsad, The effect of phenomenological $\Lambda\alpha$ potentials in ${}^6_{\Lambda\Lambda}\text{He}$ hypernuclei by using modern $\Lambda\Lambda$ potential derived from lattice QCD, *Iran. J. Phys. Res.* **22**, 701 (2023).
- [10] F. Etminan and A. Aalimi, Examination of the $\phi - NN$ bound-state problem with lattice QCD $N - \phi$ potentials, *Phys. Rev. C* **109**, 054002 (2024).
- [11] H. Le, J. Haidenbauer, U.-G. Meißner, and A. Nogga, Implications of an increased Λ -separation energy of the hypertriton, *Phys. Lett. B* **801**, 135189 (2020).
- [12] J. Haidenbauer, U.-G. Meißner, A. Nogga, and H. Polinder, The hyperon-nucleon interaction: Conventional versus effective field theory approach, in *Topics in Strangeness Nuclear Physics*, edited by P. Bydžovský, J. Mareš, and A. Gal (Springer Berlin Heidelberg, Berlin, Heidelberg, 2007) pp. 113–140.
- [13] H. Polinder, J. Haidenbauer, and U.-G. Meißner, Hyperon–nucleon interactions—a chiral effective field theory approach, *Nucl. Phys. A* **779**, 244 (2006).
- [14] S. Aoki and T. Doi, Lattice QCD and Baryon-Baryon Interactions: HAL QCD Method, *Front. Phys.* **8**, 10.3389/fphy.2020.00307 (2020).
- [15] E. Botta, T. Bressani, and A. Feliciello, On the binding energy and the charge symmetry breaking in $A \leq 16$ Λ - hypernuclei, *Nucl. Phys. A* **960**, 165 (2017).
- [16] M. Jurič *et al.*, A new determination of the binding energy values of the light hypernuclei ($A \leq 5$), *Nucl. Phys. B* **52**, 1 (1973).

- [17] A. Esser *et al.* (A1 Collaboration), Observation of ${}^4_{\Lambda}H$ hyperhydrogen by decay-pion spectroscopy in electron scattering, *Phys. Rev. Lett.* **114**, 232501 (2015).
- [18] F. Schulz *et al.*, Ground-state binding energy of ${}^4_{\Lambda}H$ from high-resolution decay-pion spectroscopy, *Nucl. Phys. A* **954**, 149 (2016), recent Progress in Strangeness and Charm Hadronic and Nuclear Physics.
- [19] S. Cho, T. Hyodo, D. Jido, C. M. Ko, S. H. Lee, S. Maeda, K. Miyahara, K. Morita, M. Nielsen, A. Ohnishi, *et al.*, Exotic hadrons from heavy ion collisions, *Prog. Part. Nucl. Phys.* **95**, 279 (2017).
- [20] E. Garrido, A. Kievsky, M. Gattobigio, M. Viviani, L. E. Marcucci, R. Del Grande, L. Fabbietti, and D. Melnichenko, $p\Lambda$ and $pp\Lambda$ correlation functions, *Phys. Rev. C* **110**, 054004 (2024).
- [21] Y. Hu, Measurements of $p - \Lambda$ and $d - \Lambda$ correlations in 3 GeV Au+Au collisions at STAR (2023), [arXiv:2401.00319](https://arxiv.org/abs/2401.00319) [nucl-ex].
- [22] K. Morita *et al.*, Probing multistrange dibaryons with proton-omega correlations in high-energy heavy ion collisions, *Phys. Rev. C* **94**, 031901 (2016).
- [23] M. Viviani, S. König, A. Kievsky, L. E. Marcucci, B. Singh, and O. V. Doce, Role of three-body dynamics in nucleon-deuteron correlation functions, *Phys. Rev. C* **108**, 064002 (2023).
- [24] S. Acharya *et al.* (ALICE Collaboration), Exploring the Strong Interaction of Three-Body Systems at the LHC, *Phys. Rev. X* **14**, 031051 (2024).
- [25] S. Bazak and S. Mrówczyński, Production of 4Li and $p-{}^3He$ correlation function in relativistic heavy-ion collisions, *Eur. Phys. J. A* **56**, 193 (2020).
- [26] S. Mrówczyński and P. Słoń, Hadron-deuteron correlations and production of light nuclei in relativistic heavy-ion collisions, *Acta Phys. Pol. B* **51**, 1739 (2020).
- [27] J. Haidenbauer, Exploring the Λ -deuteron interaction via correlations in heavy-ion collisions, *Phys. Rev. C* **102**, 034001 (2020).
- [28] K. Ogata, T. Fukui, Y. Kamiya, and A. Ohnishi, Effect of deuteron breakup on the deuteron- Ξ correlation function, *Phys. Rev. C* **103**, 065205 (2021).
- [29] L. Zhang, S. Zhang, and Y.-G. Ma, Production of ΩNN and $\Omega\Omega N$ in ultra-relativistic heavy-ion collisions, *Eur. Phys. J. C* **82**, 1 (2022).
- [30] F. Etminan, Z. Sanchuli, and M. M. Firoozabadi, Geometrical properties of ΩNN three-body states by realistic NN and first principles Lattice QCD ΩN potentials, *Nucl. Phys. A* **1033**,

- 122639 (2023).
- [31] A. Jinno, Y. Kamiya, T. Hyodo, and A. Ohnishi, Femtoscopic study of the $\Lambda\alpha$ interaction, *Phys. Rev. C* **110**, 014001 (2024).
- [32] Y. Kamiya, A. Jinno, T. Hyodo, and A. Ohnishi, Theoretical study on $\Xi\alpha$ correlation function (2024), [arXiv:2409.13207 \[nucl-th\]](#).
- [33] F. Etminan, Femtoscopic study of the $\Omega\alpha$ interaction in heavy-ion collisions (2024), [arXiv:2409.19705 \[nucl-th\]](#).
- [34] F. Etminan, Exploring the ϕ - α interaction via femtoscopic study (2024), [arXiv:2410.22756 \[nucl-th\]](#).
- [35] K. S. Myint and Y. Akaishi, Double-Strangeness Five-Body System, *Prog. Theor. Phys.* **117**, 251 (1994).
- [36] S. Acharya *et al.* (A Large Ion Collider Experiment Collaboration), First observation of an attractive interaction between a proton and a cascade baryon, *Phys. Rev. Lett.* **123**, 112002 (2019).
- [37] E. Hiyama *et al.*, Possible lightest Ξ hypernucleus with modern ΞN interactions, *Phys. Rev. Lett.* **124**, 092501 (2020).
- [38] A. Ohnishi, K. Morita, K. Miyahara, and T. Hyodo, Hadron-hadron correlation and interaction from heavy-ion collisions, *Nucl. Phys. A* **954**, 294 (2016).
- [39] Y. Kurihara, Y. Akaishi, and H. Tanaka, Effect of Λ -N repulsive core on pionic decay of ${}^5_{\Lambda}\text{He}$, *Phys. Rev. C* **31**, 971 (1985).
- [40] R. Dalitz, R. Herndon, and Y. Tang, Phenomenological study of s-shell hypernuclei with ΛN and ΛNN potentials, *Nucl. Phys. B* **47**, 109 (1972).
- [41] T. O. Yamamoto *et al.* (J-PARC E13 Collaboration), Observation of Spin-Dependent Charge Symmetry Breaking in ΛN Interaction: Gamma-Ray Spectroscopy of ${}^4_{\Lambda}\text{He}$, *Phys. Rev. Lett.* **115**, 222501 (2015).
- [42] F. Etminan and M. M. Firoozabadi, Simple Woods-Saxon type form for $\Omega\alpha$ and $\Xi\alpha$ interactions using folding model, *Chin. Phys. C* **44**, 054106 (2020).
- [43] C. Ciofi degli Atti, Electron scattering by nuclei, *Prog. Part. Nucl. Phys.* **3**, 163 (1980).
- [44] M. M. Nagels, T. A. Rijken, and J. J. de Swart, Baryon-baryon scattering in a one-boson-exchange-potential approach. II. Hyperon-nucleon scattering, *Phys. Rev. D* **15**, 2547 (1977).

- [45] P. M. M. Maessen, T. A. Rijken, and J. J. de Swart, Soft-core baryon-baryon one-boson-exchange models. II. Hyperon-nucleon potential, *Phys. Rev. C* **40**, 2226 (1989).
- [46] P. A. Zyla and others (Particle Data Group), Review of Particle Physics, *Prog. Theor. Exp. Phys.* **2020**, 083C01 (2020), https://academic.oup.com/ptep/article-pdf/2020/8/083C01/34673740/rpp2020-vol2-2015-2092_18.pdf.
- [47] M. Wang, G. Audi, F. G. Kondev, W. J. Huang, S. Naimi, and X. Xu, The AME2016 atomic mass evaluation (II). Tables, graphs and references, *Chin. Phys. C* **41**, 030003 (2017).
- [48] S. E. Koonin, Proton pictures of high-energy nuclear collisions, *Phys. Lett. B* **70**, 43 (1977).
- [49] S. Pratt, Pion interferometry of quark-gluon plasma, *Phys. Rev. D* **33**, 1314 (1986).
- [50] K. Morita, T. Furumoto, and A. Ohnishi, $\Lambda\Lambda$ interaction from relativistic heavy-ion collisions, *Phys. Rev. C* **91**, 024916 (2015).
- [51] L. Fabbietti, V. M. Sarti, and O. V. Doce, Study of the Strong Interaction Among Hadrons with Correlations at the LHC, *Annu. Rev. Nucl. Part. Sci.* **71**, 377 (2021).
- [52] S. Mrówczyński and P. Słoń, Deuteron-deuteron correlation function in nucleus-nucleus collisions, *Phys. Rev. C* **104**, 024909 (2021).
- [53] D. Mihaylov, V. Sarti, O. Arnold, L. Fabbietti, B. Hohlweger, and A. Mathis, A femtoscopic Correlation Analysis Tool using the Schrödinger equation (CATS), *Eur. Phys. J. C* **78** (2018).
- [54] D. Mihaylov and J. González González, Novel model for particle emission in small collision systems, *Eur. Phys. J. C* **83**, 590 (2023).